Supplemental Figures

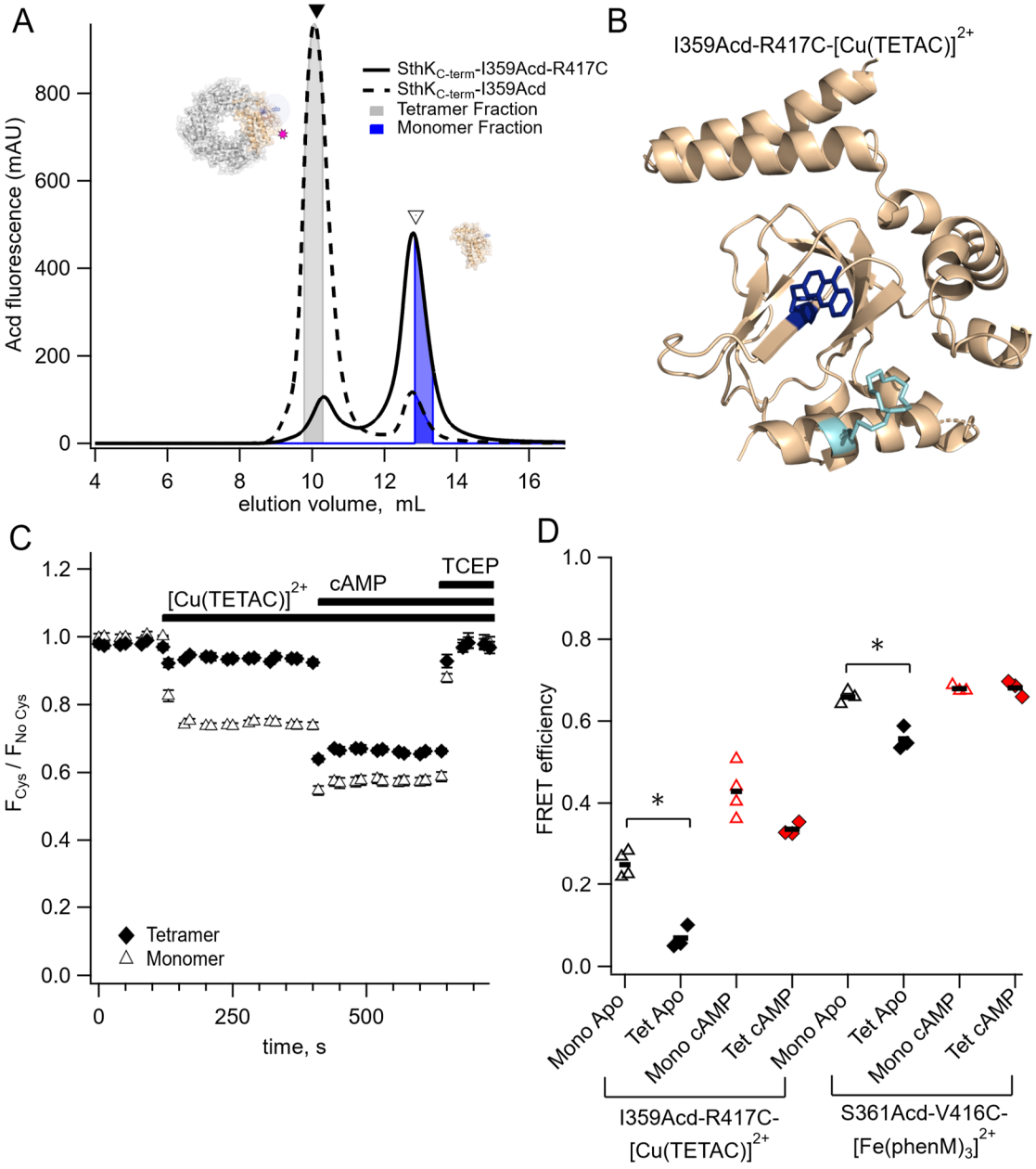

Fig. S1. Steady-state tmFRET of monomeric and tetrameric SthK$_{C\text{-}term}$. **(A)** SEC chromatogram showing separation of monomeric (empty triangle, blue area) and tetrameric protein (solid triangle, gray area) fractions for SthK$_{C\text{-}term}$-I359Acd and SthK$_{C\text{-}term}$-I359Acd-R417C (no WT SthK$_{C\text{-}term}$ present) on a Superdex 75 increase 10/300 column (GE Healthcare). **(B)** Structure showing SthK$_{C\text{-}term}$-I359Acd with [Cu(TETAC)]$^{2+}$ acceptor at R417C (PDB:4D7T). **(C)** Fluorescence time-course of SthK$_{C\text{-}term}$-I359Acd-417C upon addition of [Cu(TETAC)]$^{2+}$, cAMP and TCEP in tetrameric protein (closed diamonds) and monomeric protein (open triangles). **(D)** Summary of FRET efficiencies for monomer and tetramer, with mean values shown as horizontal lines. Left: SthK$_{C\text{-}term}$-I359Acd-R417C-[Cu(TETAC)]$^{2+}$ (apo, *P=0.0005, cAMP, P=0.06). Right: SthK$_{C\text{-}term}$-S361Acd-V416C-[Fe(phenM)$_3$]$^{2+}$ apo, *P=0.006, cAMP: P=0.9).

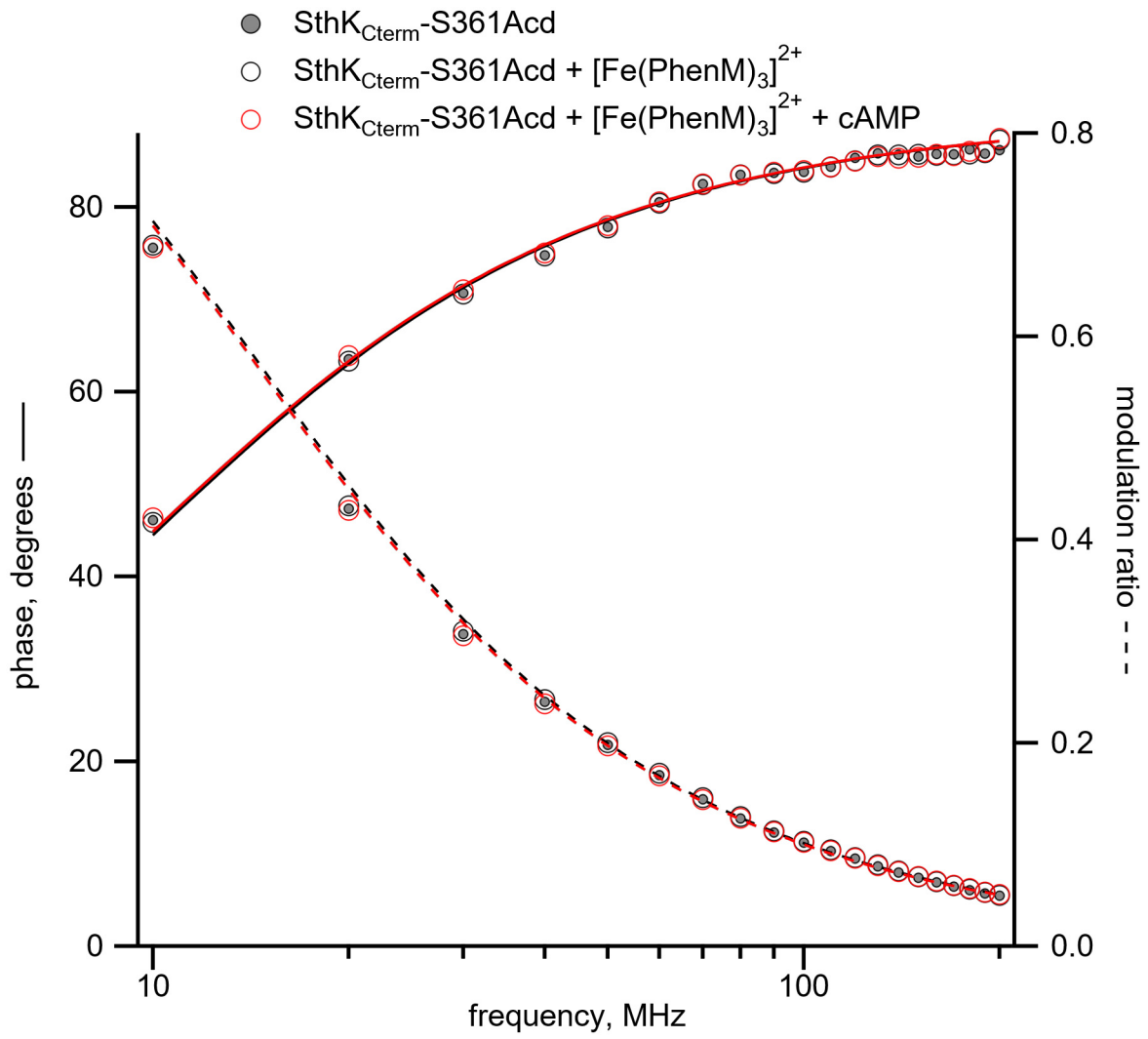

Fig. S2. Representative Weber plot of measured lifetimes of SthK$_{C\text{-}term}$-S361Acd donor-only (grey), then in the presence of [Fe(phenM)$_3$]$^{2+}$ (black), and after the addition of 1.23 mM cAMP (red), showing no change in lifetimes in the absence of a cysteine residue.

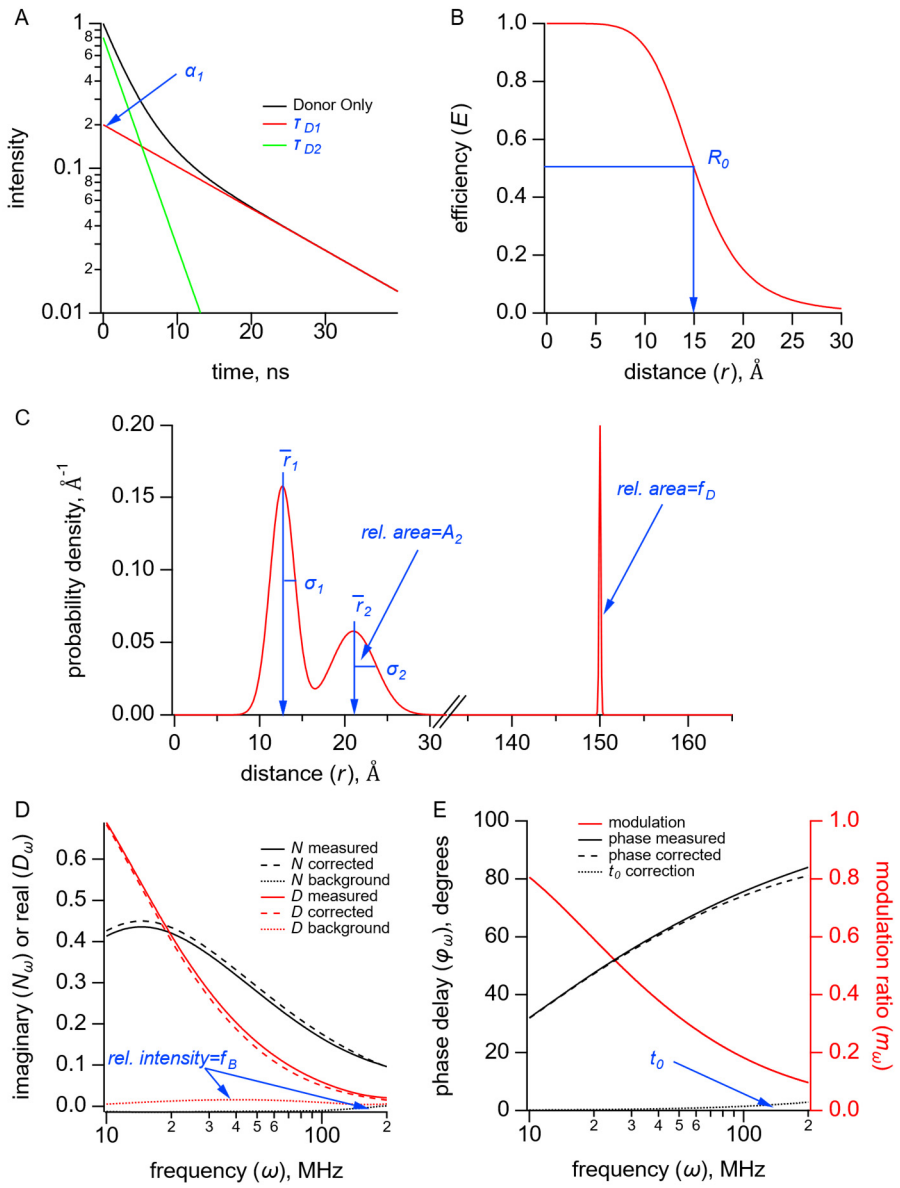

Fig. S3. Parameters used in the lifetimes fitting model for both the single and sum of two Gaussian approaches, shown in blue. **(A)** Graph of donor-only fluorescence-lifetime decay with two exponential components with time constants (τ_{D1}, τ_{D2}) **(B)** FRET efficiency (E) plot as a function of distance (r) between donor and acceptor and the R_0 values for 50% FRET transfer. **(C)** Probability distribution plot of donor and acceptor distances P(r) showing the sum of two Gaussian distributions, each with their own average distance ($\bar{r}_1$ and $\bar{r}_2$), standard deviations (σ_1 and σ_2) and relative amplitude of the second component (A_2). The donor-only fraction (f_D) is modeled as a narrow Gaussian with mean distance of 150 Å and standard deviation of 0.1 Å, beyond a detectable amount of FRET. **(D)** The in-phase (D_ω) and out-of-phase (N_ω) components are plotted for the measured, corrected, and background fluorescence signal as a function of the excitation modulation frequency (ω), where f_B is the fraction of the fluorescence intensity due to the background. **(E)** Plot of the phase delay (φ_ω) and modulation ratio (m_ω) of the measured and corrected fluorescence response as a function of the modulation frequency (ω) where t_0 is the time shift of the instrument response function.

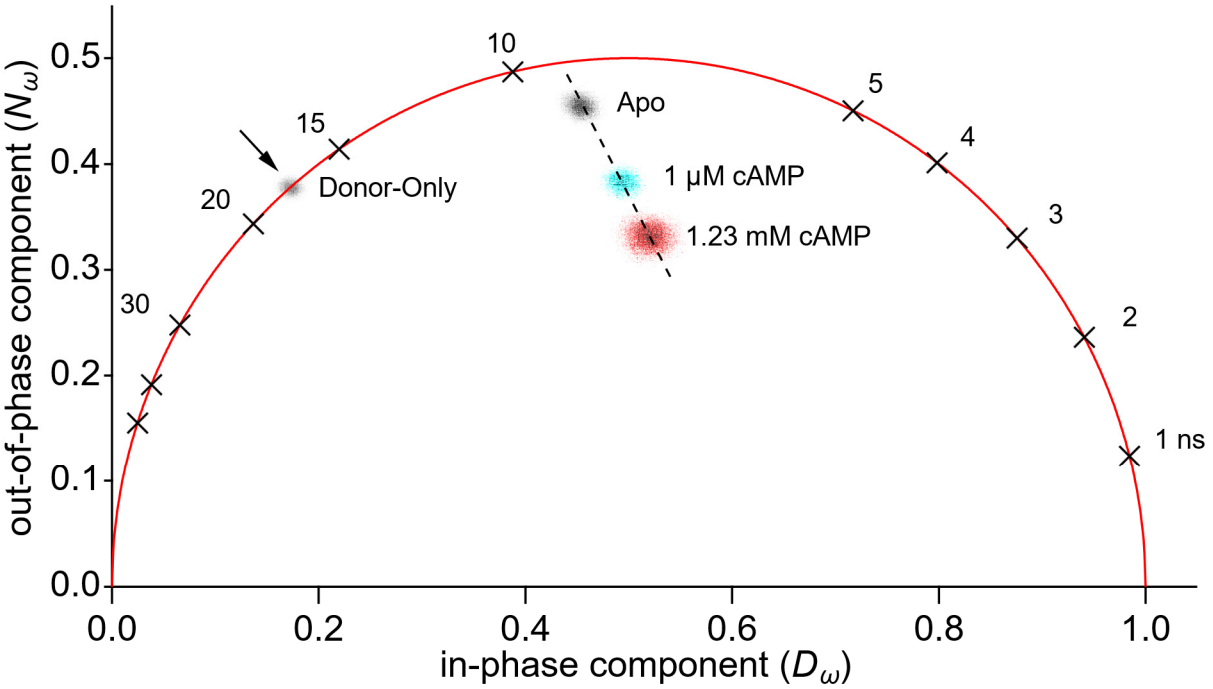

Fig. S4. Representative phasor plot of measured lifetimes of $SthK_{C\text{-}term}$-S361Acd-V416C alone (donor-only, grey), in the presence of $[Ru(bpy)_2phenM]^{2+}$ (apo, black), in the presence of 1 µM cAMP (cyan) and presence of 1.23 mM cAMP (red).

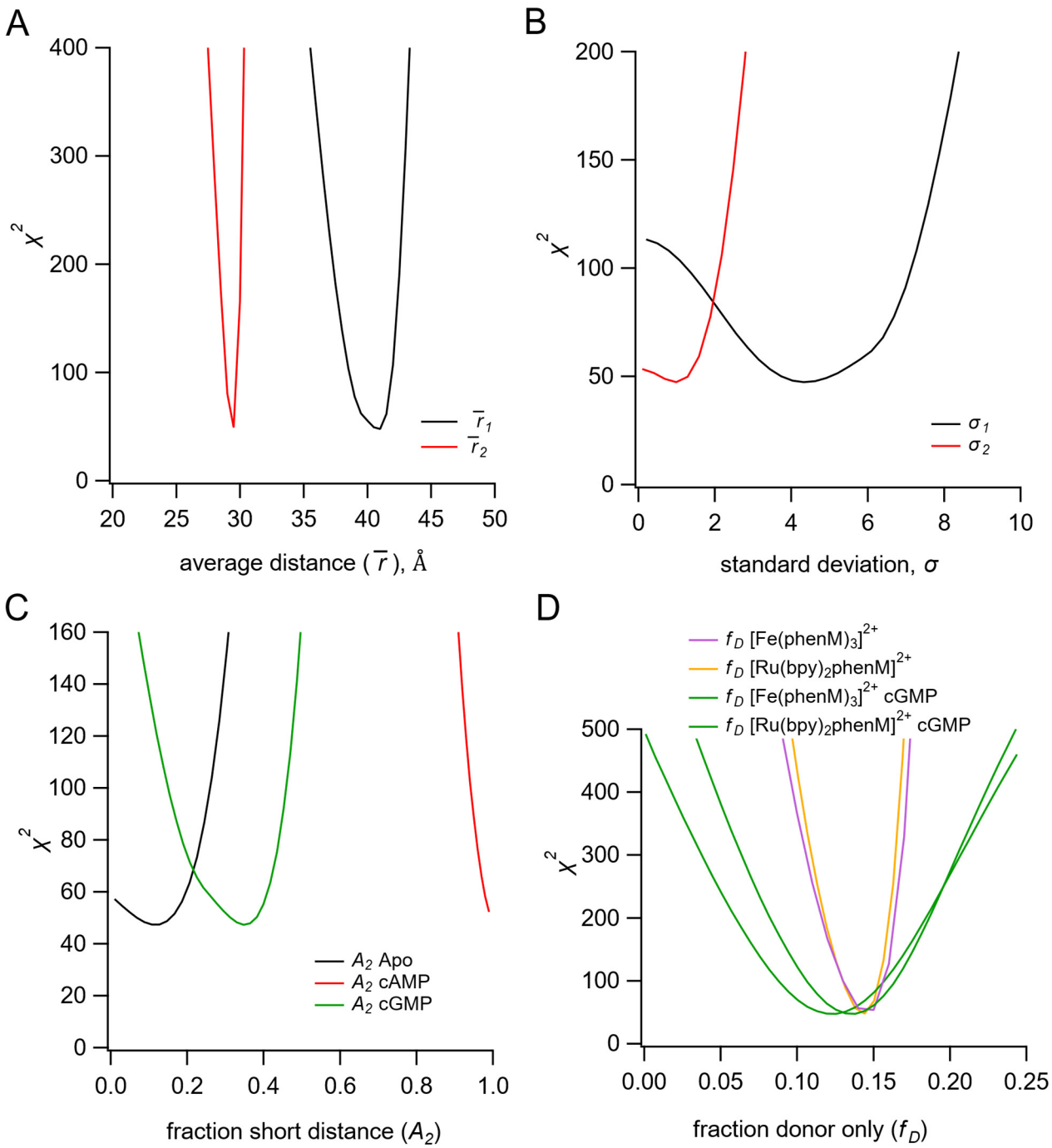

Fig. S5. Identifiability of parameters in the sum of two Gaussian distributions model, with global fitting Fe(phenM)$_3$]$^{2+}$ and [Ru(bpy)$_2$phenM]$^{2+}$ data. **(A-B)** Minimization of χ^2 values for the Gaussian average distance ($\bar{r}$) (A) and standard deviation (σ) (B) for the resting (black) and active states (red). **(C)** Minimization of χ^2 values for parameter A_2 for the conditions of apo, cAMP and cGMP. **(D)** Minimization of χ^2 values for the fraction of donor-only component (f_D) in protein samples for each experiment of apo and cAMP for [Fe(phenM)$_3$]$^{2+}$, of apo and cAMP for [Ru(bpy)$_2$phenM]$^{2+}$, of cGMP for [Fe(phenM)$_3$]$^{2+}$, and of cGMP for [Ru(bpy)$_2$phenM]$^{2+}$.